

## Magmatic ferromagnesian inclusions in granitoid plagioclase cores, Barrington Tops Granodiorite, New South Wales, Australia

DOUGLAS R. MASON

Department of Geology, University of Newcastle, New South Wales 2308, Australia

### ABSTRACT

Small inclusions of hypersthene, augite, hornblende, and Fe-Ti oxides occur in plagioclase cores of granitoids from the Permian Barrington Tops Granodiorite, New South Wales. Mineralogically and chemically the ferromagnesian inclusions match larger discrete grains in the granitoids. Pyroxenes of both parageneses yield temperatures ranging from ~1000 to <500°C, indicating partial equilibration of these magmatic phases during slow cooling. A magmatic origin for the ferromagnesian inclusions demands a similar origin for their plagioclase host material. Plagioclase cores, therefore, cannot be used as unequivocal evidence of restite (residual high-grade metamorphic source material) in discussions of granitoid genesis. The Barrington Tops Granodiorite crystallized from silicate liquid with little or no restite entrained from the source.

### INTRODUCTION

In many granitoid rocks, plagioclase crystals contain euhedral to subrounded cores that may display mottled extinction, partial alteration, and fracturing. Piwinski (1968) concluded that such plagioclase cores in granitoids of the Sierra Nevada batholith were residual high-grade metamorphic material ("restite"), entrained in granitic melt from a deeper crustal source region. More recently, proponents of the "restite theory" for granitoid genesis continue to suggest that the plagioclase cores represent restite material (White and Chappell, 1977; Chappell, 1978).

Less commonly, the plagioclase cores may contain small inclusions of ferromagnesian minerals. Although this textural phenomenon has been briefly recorded (Piwinski, 1968; Vernon and Flood, 1982; Vernon, 1983), no detailed studies are available. Clearly, if the host plagioclase cores represent restite, then their ferromagnesian inclusions must also have a similar (metamorphic) origin. On the other hand, if the inclusions are magmatic, then their plagioclase host material must also be magmatic and may not be used in support of the "restite theory" for granitoid genesis.

In this paper, examples of mineral inclusions in granitoid plagioclase cores are studied from the Permian Barrington Tops Granodiorite, New South Wales (Fig. 1). Data from petrography, mineral chemistry, and thermometry indicate a magmatic origin for the ferromagnesian inclusions, with consequent implications for the genesis of these rocks in particular and granitoids in general.

### PREVIOUS WORK

Mason and Kavalieris (1984) presented the first geologic map of the Barrington Tops Granodiorite, together with preliminary petrographic and chemical data for the prin-

cipal rock types and minerals. They demonstrated that the Permian intrusive complex comprises three separate plutons emplaced at shallow crustal levels within virtually unmetamorphosed Carboniferous and Devonian sedimentary rocks of the Tamworth synclinal zone of the New England fold belt in northeastern New South Wales. Two medium-grained massive granitoid rock types predominate in the complex: biotite-hornblende granodiorite and hypersthene-augite granodiorite.

Eggs (1984) obtained geochemical data for one pluton of the complex, and Hensel et al. (1985) included one sample in their isotopic study of the New England batholithic rocks.

### MATERIALS AND METHODS

One representative sample of each dominant rock type was selected for detailed study. Petrographic studies were followed by electron-microprobe analysis of mineral phases using a JEOL JXA-50A scanning-electron microscope fitted with an EDAX 183 energy-dispersive detector and data reduction following Reed and Ware (1975). Analytical conditions were accelerating voltage, 15 kV; electron-beam diameter, ~0.5  $\mu\text{m}$ ; specimen current, 1.70–1.80 nA. Estimates of pyroxene equilibration temperatures were made using the geothermometer of Lindsley and Andersen (1983) and Lindsley (1983).

For comparative purposes, similar studies were conducted on a pyroxene dacite lava from the Carboniferous sequence of the Hunter Valley (Wilkinson, 1971). Plagioclase phenocrysts of some of these calc-alkaline volcanics contain mottled cores with abundant ferromagnesian inclusions (Vernon, 1983, Fig. 1), similar in many respects to the texture observed in granitoids. Although there might always be some doubt concerning the proportions of silicate liquid and crystals in granitoid magmas, there can be little doubt that most lavas have crystallized from magmatic systems composed largely of silicate liquid. It is of direct interest, therefore, to compare the results of the parallel studies on the granitoid and volcanic rocks.

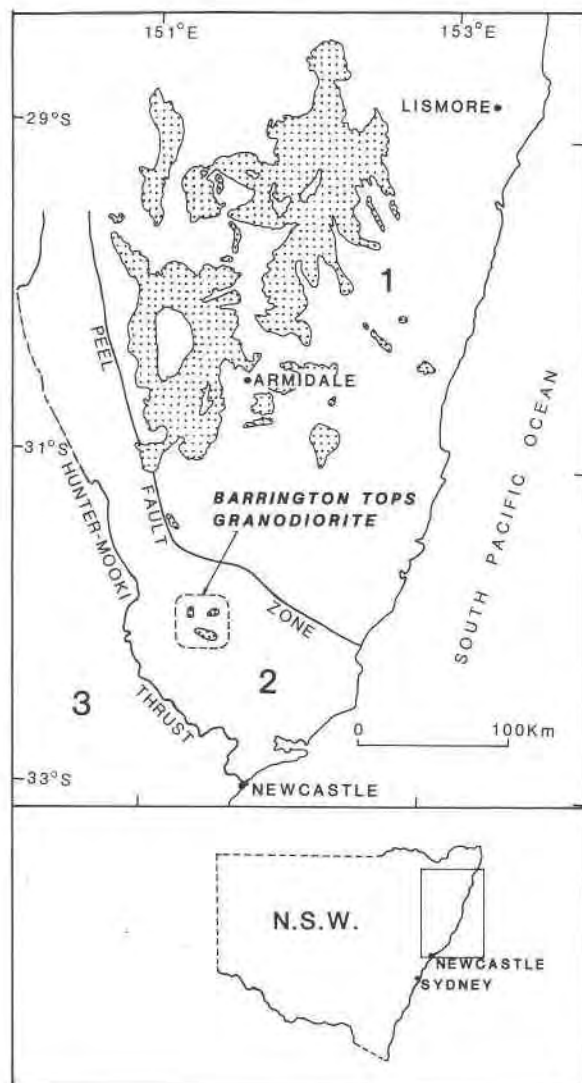


Fig. 1. Geologic sketch map showing location of the Barrington Tops Granodiorite and other Permian-Triassic granitoids (stippled pattern) in northeastern New South Wales. 1 = New England fold belt, 2 = Tamworth synclinal zone, 3 = Sydney basin.

## RESULTS

### Petrography of the granitoids

**Hypersthene-augite granodiorite.** This is a waxy-gray massive rock, which, in thin section, displays an even-grained, hypidiomorphic granular texture with plagioclase prisms (approximately 48 vol%) up to 4.5 mm long. Quartz (15%) forms large anhedral patches molded on plagioclase and ferromagnesian minerals. Interstitial orthoclase (12%) is in places micrographically intergrown with quartz. Faintly pleochroic hypersthene prisms (12%), subhedral augite grains (8%), and Fe-Ti oxide euhedra (2%) form aggregates as well as discrete grains. Ragged biotite flakes ( $\alpha$  = pale yellow,  $\beta$  =  $\gamma$  = tan brown) are molded on other ferromagnesian minerals. Small apatite prisms are present in trace amounts. Optical evidence of deuteritic alteration

Table 1. Some petrologic features of the granitoids

Feature	BT.50 (Hyp-Aug granodiorite)	BT.2 (Bt-Hbl granodiorite)
	Plagioclase	
Size (mm)	4.5	4.0
Core composition* (mol%)	An <sub>76-33</sub>	An <sub>70-33</sub>
Rim composition* (mol%)	An <sub>64-19</sub>	An <sub>42-19</sub>
	Ferromagnesian phases**	
Larger discrete grains	Opx, Cpx, Mag, Bt	(Cum), Cpx, Hbl, Mag, Bt
Inclusions in plag cores	Opx, Cpx, Mag	Opx, Cpx, Hbl, Mag
	Bulk-rock chemistry	
SiO <sub>2</sub> (wt%)	63.78	61.54
Na <sub>2</sub> O/K <sub>2</sub> O	1.91	2.23
Mol. MgO/(MgO + total FeO)	0.47	0.43
Mol. Al <sub>2</sub> O <sub>3</sub> /(Na <sub>2</sub> O + K <sub>2</sub> O + CaO)	0.93	0.85
K/Rb	224	321
Rb/Sr	0.16	0.13

\* Compositions by EPMA (see text for instrumental conditions).

\*\* Mineral abbreviations after Kretz (1983).

is very limited: trace amounts of chlorite occur in biotite, sericite in plagioclase, and clay minerals in orthoclase.

**Biotite-hornblende granodiorite.** In hand specimen this is a massive, speckled white and black rock, which, in thin section, displays a hypidiomorphic granular texture with plagioclase prisms (approximately 55 vol%) up to 4 mm long. Quartz (15%) and orthoclase (10%) occur as anhedral or angular interstitial patches. Subhedral hornblende (8%;  $\alpha$  = greenish yellow,  $\beta$  = green,  $\gamma$  = bluish green) commonly contains cores of fretted augite (3%) or colorless twinned cummingtonite (2%) peppered with minute opaque oxide grains. The low-Ca amphibole is presumably after primary orthopyroxene. Biotite (5%;  $\alpha$  = yellow,  $\beta$  =  $\gamma$  = very dark reddish brown) forms discrete plates, but also commonly occurs as smaller grains within or marginal to other ferromagnesian minerals that, in places, tend to occur as anhedral grains in clots up to 5 mm in diameter. Accessory phases include apatite and zircon. Deuteritic alteration minerals are present in trace amounts and are similar to those mentioned above for the hypersthene-augite granodiorite.

### Petrography of ferromagnesian inclusions in plagioclase

In both principal rock types, plagioclase crystals commonly display mottled cores mantled by clear, normally zoned rims (Table 1).

In many cases the cores contain small ferromagnesian mineral inclusions ranging from 0.05 to 0.50 mm in size (Fig. 2). Opaque oxide inclusions are euhedral whereas the silicate phases form subhedral to subrounded equant prisms or blebs. It is important to observe that those phases present as inclusions are also present as larger discrete grains in the rocks (Table 1). Exsolution lamellae are absent from the inclusion pyroxenes, an observation that also applies to the larger pyroxenes. Very thin fringes of

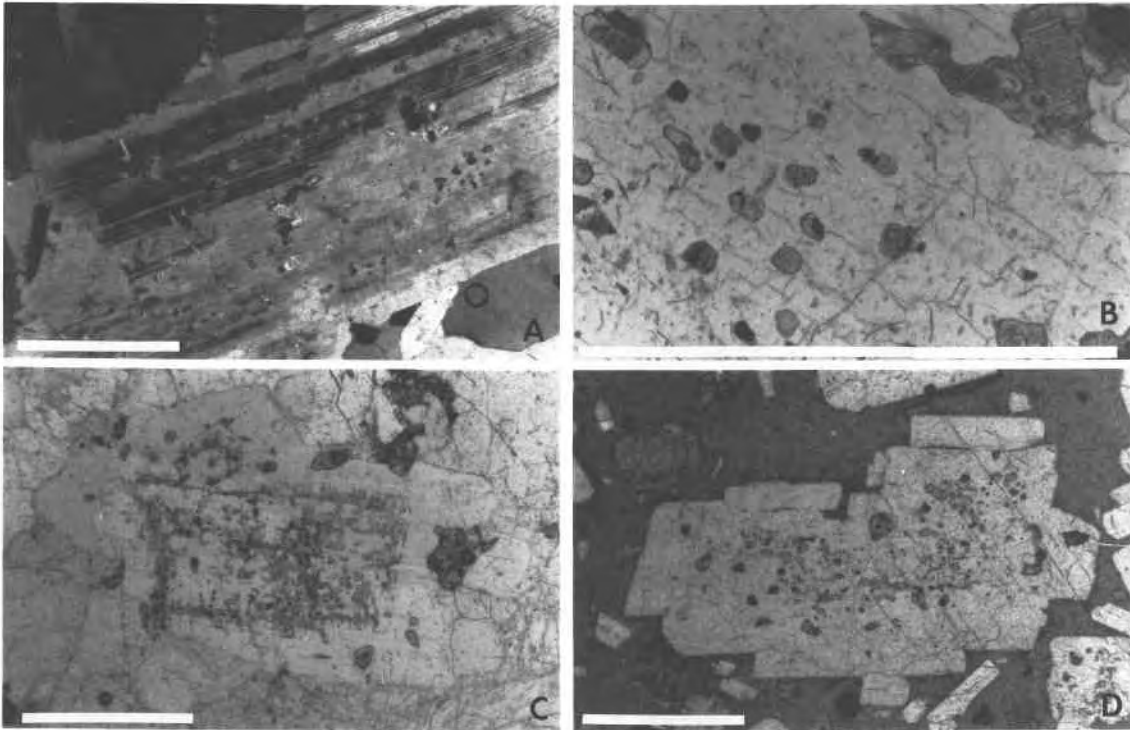


Fig. 2. Photomicrographs of ferromagnesian inclusions in plagioclase cores. (A) Scattered inclusions in mottled core region of plagioclase prism (BT.2, biotite-hornblende granodiorite). Crossed polars; scale bar = 1 mm. (B) Inclusions in same grain as (A), showing Fe-Ti oxide and pyroxene in places mantled by secondary actinolitic amphibole. Plane-polarized light; scale bar = 1 mm. (C) Polycrystalline plagioclase grain with small inclusions in sericitized core region (mottled under crossed polars) and larger inclusions in rim zone. Plane-polarized light; scale bar = 1 mm. (BT.50, hypersthene-augite granodiorite). (D) Pyroxene and Fe-Ti oxide inclusions in core region of plagioclase phenocryst (2017, hypersthene-augite dacite). Plane-polarized light, bar = 1 mm. The phenomenon of inclusions in plagioclase cores is similar to that observed in the plutonic rocks illustrated in (A), (B), and (C).

secondary amphibole are present around some pyroxene inclusions in the biotite-hornblende granodiorite, but are absent in the pyroxene granodiorite. In neither rock type does biotite occur as genuine inclusions in plagioclase cores, although in places tiny secondary biotite shreds are present in association with sericite at core-mantle boundaries and along fractures passing through cores.

#### Mineral chemistry

**Plagioclase.** In both rock types, plagioclase compositions display considerable variation (Table 1). Cores range from sodic bytownite to sodic andesine, but regular zoning is not apparent. Rather, patchy distribution of variable compositions is usual. Rims are normally zoned from sodic labradorite or sodic andesine to sodic oligoclase.

**Orthopyroxene.** Compositions of the orthopyroxenes are summarized in Table 2. In both rock types the large grains and small inclusions of orthopyroxene are hypersthene, but those of the hypersthene-augite granodiorite have higher  $100\text{Mg}/(\text{Mg} + \text{Fe}^{2+} + \text{Fe}^{3+} + \text{Mn})$  reflecting higher bulk-rock  $\text{Mg}/\text{Fe}_{\text{tot}}$ . In this rock type, where both large and small orthopyroxenes are preserved, there is remarkable agreement between the average compositions of the two parageneses, even to the extent of minor components such as  $\text{TiO}_2$ ,  $\text{Al}_2\text{O}_3$ ,  $\text{MnO}$ ,  $\text{Cr}_2\text{O}_3$ , and  $\text{V}_2\text{O}_5$ .

Subtle but important variations in compositions are described in the section on thermometry. In the biotite-hornblende granodiorite, addition of a petrographically reasonable amount (5%) of magnetite to the average cummingtonite composition results in a calculated primary orthopyroxene composition (analysis 5, Table 2) very close to the average orthopyroxene inclusion composition.

**Clinopyroxene.** Average clinopyroxene compositions (Table 2) fall in the salite field of the pyroxene quadrilateral, with those of the pyroxene granodiorite displaying consistently higher  $100\text{Mg}/(\text{Mg} + \text{Fe}^{2+} + \text{Fe}^{3+} + \text{Mn})$ . In addition, it should be noted that in both rock types the average clinopyroxene inclusion composition is more Fe-rich than the average composition of the large grains.

**Amphibole.** Amphibole is present only in the biotite-hornblende granodiorite. Average compositions are set out in Table 3. Primary amphibole, occurring both as large grains and small inclusions in plagioclase cores, is of magnesio-hornblende composition (Leake, 1978). Secondary actinolitic hornblende is developed as patchy replacement of primary clinopyroxene grains and as thin rims on pyroxene inclusions in plagioclase cores.

**Fe-Ti oxides.** Members of the magnetite-ulvöspinel and ilmenite-hematite solid-solution series are present in both rock types as large grains and as small inclusions in pla-

Table 2. Average pyroxene compositions

	BT.50 (hypersthene-augite granodiorite)				BT.2 (biotite-hornblende granodiorite)			
	1	2	3	4	5	6	7	8
<i>N</i>	13	9	14	7	—	7	24	19
SiO <sub>2</sub> wt% (esd)	51.37(31)	51.66(54)	52.32(70)	51.31(38)	51.56	53.08(87)	51.64(72)	51.47(76)
TiO <sub>2</sub>	0.25(7)	0.25(6)	0.21(23)	0.47(10)	0.12	n.d.	0.30	0.29(13)
Al <sub>2</sub> O <sub>3</sub>	0.63(20)	0.61(20)	0.75(67)	1.48(33)	0.44	0.23(28)	0.95(43)	0.87(32)
Cr <sub>2</sub> O <sub>3</sub>	tr.	tr.	0.21(4)	0.21(4)	0.0	n.d.	n.d.	n.d.
V <sub>2</sub> O <sub>5</sub>	tr.	tr.	tr.	tr.	tr.	n.d.	n.d.	n.d.
FeO*	25.17(49)	25.12(150)	9.41(73)	10.77(60)	29.26	28.24(73)	12.17(90)	13.01(69)
MnO	0.78(6)	0.73(10)	0.32(7)	0.37(7)	1.00	1.18(13)	0.39(9)	0.43(5)
MgO	19.76(38)	19.97(125)	13.51(28)	13.13(32)	15.65	14.13(32)	11.99(75)	11.02(35)
CaO	1.19(26)	0.99(23)	22.43(90)	21.25(70)	1.37	1.32(35)	21.69(91)	22.24(57)
Na <sub>2</sub> O	0.67(15)	0.64(13)	0.68(19)	0.82(15)	0.56	0.53(9)	0.63(9)	0.60(14)
K <sub>2</sub> O	n.d.	n.d.	n.d.	n.d.	0.0	n.d.	n.d.	n.d.
Total	99.82	99.97	99.84	99.81	99.96	98.71	99.76	99.93
				Atomic proportions				
Ca	2.4	2.0	45.9	44.1	2.9	3.0	45.0	46.3
Mg	56.2	56.7	38.5	37.9	46.5	44.6	34.6	31.9
Fe <sup>2+</sup> + Fe <sup>3+</sup> + Mn	41.4	41.2	15.6	18.0	50.5	52.4	20.4	21.8
100 Mg/(Mg + Fe <sup>2+</sup> + Fe <sup>3+</sup> + Mn)	57.6	57.9	71.2	67.7	48.0	46.0	63.0	59.4

Note: 1 = large hypersthene grains; 2 = small hypersthene inclusions in plagioclase; 3 = large augite grains; 4 = small augite inclusions in plagioclase; 5 = calculated primary orthopyroxene composition using average cummingtonite (analysis 5, Table 3) plus 5% average magnetite (analysis 6, Table 4); 6 = small hypersthene inclusions in plagioclase; 7 = large augite grains; 8 = small augite inclusions in plagioclase.

For this and subsequent tables, *N* = number of spot analyses, esd = estimated standard deviation, n.d. = not detected, tr. = trace, FeO\* = total Fe as FeO, Fe<sup>2+</sup>/Fe<sup>3+</sup> calculated from charge-balance considerations.

gioclase cores. Average compositions (Table 4) confirm extensive subsolidus equilibration. In the biotite-hornblende granodiorite, low-Ti titanomagnetite and ilmenite of both parageneses are remarkably similar in composition. In the pyroxene granodiorite, partial equilibration has produced a more variable assemblage that includes ulvöspinel lamellae in low-Ti titanomagnetite as well as titanomagnetites of varying Ti content. In both rock types, co-existing pairs of Mag-Usp<sub>ss</sub> and Ilm-Hem<sub>ss</sub> give temperatures of equilibration <500°C, according to the curves of Buddington and Lindsley (1964).

### Pyroxene thermometry

Temperatures have been estimated for the pyroxene compositions using the pyroxene thermometer of Lindsley (1983) and Lindsley and Andersen (1983). Individual spot analyses were projected onto Wo-En-Fs using the projection scheme of Lindsley (1983), and temperatures were estimated from experimentally determined isotherms projected onto Wo-En-Fs (Lindsley, 1983, Fig. 9).

Plots of spot analyses and isotherms are presented in Figures 3 and 4, and results are summarized in Table 5. Wide ranges of temperatures are evident in the granitoid

Table 3. Average amphibole compositions, biotite-hornblende granodiorite

	1	2	3	4	5
<i>N</i>	11	5	3	7	7
SiO <sub>2</sub> wt% (esd)	47.81(102)	45.56(85)	50.59(153)	50.80(17)	53.01(41)
TiO <sub>2</sub>	1.24(20)	1.20(7)	1.16(22)	0.56(20)	0.10(9)
Al <sub>2</sub> O <sub>3</sub>	4.98(57)	6.82(24)	3.48(54)	3.17(113)	0.43(19)
Cr <sub>2</sub> O <sub>3</sub>	n.d.	n.d.	n.d.	n.d.	n.d.
V <sub>2</sub> O <sub>5</sub>	0.07(7)	0.12(7)	n.d.	n.d.	n.d.
FeO*	19.20(80)	20.42(24)	15.30(61)	17.77(83)	25.28(100)
MnO	0.42(5)	0.29(5)	0.27(9)	0.38(9)	1.03(11)
MgO	11.16(66)	9.62(29)	13.63(90)	12.46(65)	16.09(49)
CaO	11.33(25)	11.88(20)	12.28(59)	11.92(69)	1.40(70)
Na <sub>2</sub> O	1.37(21)	1.35(18)	1.19(29)	0.89(17)	0.58(7)
K <sub>2</sub> O	0.51(8)	0.74(13)	0.32(4)	0.26(10)	n.d.
Total	98.09	98.00	98.22	98.21	97.92
			Atomic proportions		
Ca	27.1	28.8	28.4	27.7	3.2
Mg	37.1	32.5	43.9	40.2	51.4
Fe <sup>2+</sup> + Fe <sup>3+</sup> + Mn	35.8	38.7	27.7	32.1	45.4
100 Mg/(Mg + Fe <sup>2+</sup> + Fe <sup>3+</sup> + Mn)	50.9	45.6	61.3	55.5	53.1

Note: 1 = primary magnesio-hornblende grains; 2 = primary magnesio-hornblende inclusions in plagioclase; 3 = secondary actinolitic hornblende after clinopyroxene grains; 4 = secondary actinolitic hornblende rims on pyroxene inclusions; 5 = secondary cummingtonite after primary orthopyroxene grains.

Table 4. Average Fe-Ti oxide compositions

	BT.50 (hypersthene-augite granodiorite)					BT.2 (biotite-hornblende granodiorite)			
	1 <sup>+</sup>	2	3	4	5	6	7	8	9
N	12	3	1	7	2	3	7	3	5
SiO <sub>2</sub> wt% (esd)	tr.	tr.	tr.	n.d.	n.d.	tr.	tr.	n.d.	n.d.
TiO <sub>2</sub>	1.38(87)	15.86(289)	34.33	0.54	45.78(404)	0.30(8)	0.42(17)	48.27(32)	50.87(9)
Al <sub>2</sub> O <sub>3</sub>	0.80(22)	1.64(73)	1.51	0.57	n.d.	0.23(20)	0.31(8)	n.d.	n.d.
Cr <sub>2</sub> O <sub>3</sub>	tr.	0.30(12)	0.35	tr.	n.d.	n.d.	n.d.	n.d.	n.d.
V <sub>2</sub> O <sub>5</sub>	1.11(9)	0.89(3)	0.59	0.72(16)	0.34(15)	1.01(8)	0.88(13)	tr.	n.d.
FeO*	99.77(105)	78.36(231)	60.87	93.58(36)	51.54(196)	92.88(42)	96.00(78)	48.32(36)	48.78(47)
MnO	n.d.	0.64(11)	1.11	n.d.	0.55(9)	n.d.	n.d.	1.34(5)	1.89(53)
MgO	0.32(16)	tr.	n.d.	0.22(12)	1.04(42)	0.26(9)	tr.	n.d.	n.d.
CaO	tr.	tr.	0.25	0.26(5)	0.23(2)	n.d.	0.14(8)	n.d.	n.d.
Total	98.38	97.69	99.01	95.89	99.48	94.68	97.75	97.93	101.54
Mt (mol%)	96	44	0	98	—	99	99	—	—
Usp	4	56	100	2	—	1	1	—	—
Ilm	—	—	—	—	85	—	—	93	95
Hem	—	—	—	—	15	—	—	7	5

Note: 1 = large magnetite grains; 2 = titaniferous magnetite lamellae in large grains; 3 = ulvöspinel lamella in large grain; 4 = small magnetite grains in plagioclase cores; 5 = small ilmenite grains in plagioclase cores; 6 = large magnetite grains; 7 = small magnetite grains in plagioclase cores; 8 = large ilmenite grains; 9 = small ilmenite grains in plagioclase cores.

rocks: pyroxene inclusions in plagioclases and larger discrete pyroxene grains yield temperatures ranging from 1000 to <500°C. In comparison, a much more restricted range of temperatures is observed in the pyroxene dacite (1050–950°C).

## DISCUSSION

### Implications from petrography and mineral chemistry

The presence of numerous inclusions in the plagioclase cores militates against a high-grade metamorphic (restite) origin principally because high-grade metamorphism of suitable basic source rocks results in granoblastic textures characterized by inclusion-free plagioclase (Vernon, 1968, 1970; Spry, 1969). In lower-grade metamorphic rocks, amphibole may be present as oriented acicular inclusions in plagioclase and as rare euhedral inclusions at higher grades. However, pyroxene inclusions are conspicuously absent in published descriptions of high-grade metamorphic plagioclases. It appears that it is extremely difficult for pyroxene to nucleate or be trapped within plagioclase under high-grade metamorphic conditions. On the other hand, pyroxene inclusions are well-known in plagioclase of undoubted magmatic origin (e.g., in plagioclase of some basalts).

It might be argued that the inclusions represent subsequently crystallized melt that infiltrated plagioclase reabsorption cavities. If this were the case, the inclusions should be polycrystalline, polymineralic aggregates, representative of the bulk melt composition. Instead, the inclusions are discrete subhedral crystals indicative of independent nucleation and growth in liquid.

The textural evidence, therefore, favors a magmatic origin for the plagioclase cores and their ferromagnesian inclusions.

Of further interest is the observation that the ferromagnesian phases occurring as inclusions also occur as larger discrete grains. This mineralogical match could be explained by either of two processes: (1) magmatic crys-

tallization of both parageneses from melt of the same or similar composition or (2) complete equilibration of restite (host plagioclase plus inclusions) with silicate liquid. The latter process would have resulted in recrystallized, metamorphic textures that are not observed in these rocks.

The close chemical similarity of matching ferromagnesian phases also may be explained by either the magmatic or equilibrated restite hypothesis. For example, the orthopyroxenes of the pyroxene granodiorite (analyses 1 and 2, Table 2) are virtually identical. If the inclusions were restite, and equilibration had occurred between them and silicate liquid, it is difficult to imagine transport mechanisms that operated so efficiently as to ensure coincidence of compositions of orthopyroxene crystallizing from the magma and restite orthopyroxene modified by reaction with the melt. The pyroxene inclusions would have been completely enclosed by plagioclase, and could have communicated with the melt only by solid diffusion through plagioclase or by fluid-phase transport along plagioclase cleavages and fractures. Such processes are highly unlikely to account for the closely similar abundances of the ferromagnesian minerals' minor elements (Ti, V, Cr, Mn) in particular. Slight differences in average compositions between inclusions and larger discrete grains are most simply explained by slight changes in liquid composition or activities of volatile species accompanying progressive magmatic crystallization. Thus, slightly higher 100Mg/(Mg + Fe<sup>2+</sup> + Fe<sup>3+</sup> + Mn) in large grains compared with inclusions may be attributed to increasing *f*<sub>O<sub>2</sub></sub> during crystallization (Czamanske and Wones, 1973; Mason, 1978).

### Evaluation of pyroxene thermometry

**Analytical accuracy of minor components.** It is possible that the wide range in temperatures of the granitoid pyroxenes might be due, in part, to analytical inaccuracies, especially for the minor components. An assessment of overestimation and underestimation of Al<sub>2</sub>O<sub>3</sub>, TiO<sub>2</sub>, Na<sub>2</sub>O, and Fe<sup>3+</sup> was made by selecting a single augite analysis,

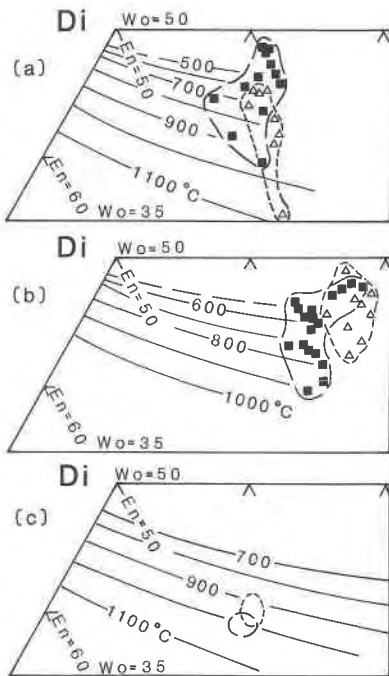


Fig. 3. Projection of clinopyroxene compositions into portion of Wo-En-Fs, with experimental isotherms (from Lindsley, 1983). (A) BT.50, pyroxene granodiorite; (B) BT.2, biotite-hornblende granodiorite; (C) 2017, pyroxene dacite. ■ = large grains; △ = inclusions; long dashed field = large grains; short dashed field = inclusions.

successively adding and subtracting reasonable amounts of each minor component, and redetermining the temperature. The results are depicted in Figure 5. Overestimation or underestimation of a single component would result in a temperature change on the order of  $\pm 50^\circ\text{C}$ . Comparison of the pyroxene data of this work with data of Wilkinson (1971) suggests a slight overestimation of temperatures by approximately  $10\text{--}20^\circ\text{C}$ . The worst cases would arise for covariation of  $\text{Al}_2\text{O}_3$  and  $\text{Fe}^{3+}$  with antipathetic variation of  $\text{Na}_2\text{O}$  and  $\text{TiO}_2$ , when temperature discrepancies of about  $\pm 100^\circ\text{C}$  would result. Covariations other than these would result in temperature changes ranging from zero to less than  $100^\circ\text{C}$ . It is apparent that the effects of inaccuracies of minor components are not sufficiently great to change an important conclusion of this work, namely that liquidus temperatures are retained in some of the pyroxenes.

**Applicability of pyroxene thermometry.** It is relevant to inquire whether the pyroxene thermometer, derived from experimental work in a synthetic system, can be applied to the natural pyroxenes of this work. Lindsley (1983) wisely discouraged application of his thermometer to pyroxenes containing  $> 10$  mol% of non-quadrilateral components (i.e., components other than Wo, En, and Fs). The granitoid pyroxenes of this work contain 3–16% “others.” Although some of these compositions exceed the suggested limit, there is no observed correlation of tem-

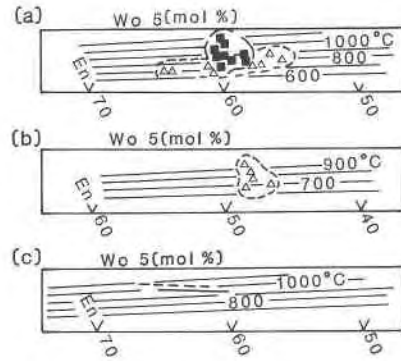


Fig. 4. Projection of orthopyroxene compositions into portion of Wo-En-Fs, with experimental isotherms (from Lindsley, 1983). (A) BT.50, pyroxene granodiorite. (B) BT.2, biotite-hornblende granodiorite. (C) 2017, pyroxene dacite. Symbols as for Fig. 3.

perature and “others.” Thus, for the pyroxene granodiorite, a plot of estimated temperature against mole percentage of “others” in the pyroxenes yields a correlation coefficient  $r = 0.219$ . It may safely be concluded that variation in minor components of these pyroxenes does not control the observed temperature variation.

**Interpretation.** The interpretation of pyroxene thermometry for the pyroxene dacite is quite straightforward. The high temperatures ( $\sim 1000^\circ\text{C}$ ) are compatible with a magmatic origin and compare favorably with an independent temperature estimate using coexisting Fe-Ti oxides (Wilkinson, 1971; also see Table 5). The restricted range in composition (and hence estimated temperatures) is explained by rapid quenching of the dacite lava, effectively “freezing in” the magmatic compositions and temperature. There was no opportunity for subsequent equilibration processes to change the original magmatic compositions.

By analogy, the wide range in temperatures indicated by the granitoid pyroxenes is most simply interpreted as the result of variable degrees of intracrystal equilibration of high-temperature magmatic pyroxenes, during slow cooling of the Barrington Tops plutons. The maximum temperatures ( $\sim 1000^\circ\text{C}$ ) are broadly in accord with liquidus temperatures of granodioritic magmas (Wyllie, 1977) and are considerably higher than maximum temperatures estimated for high-grade metamorphic terrains ( $\sim 850\text{--}$

Table 5. Summary of equilibration temperatures ( $^\circ\text{C}$ ) from pyroxene thermometry

	BT.2 Bt-Hbl grano- diorite	BT.50 Hyp-Aug grano- diorite	2017 Hyp-Aug dacite
Large grains of Cpx	925–<500	975–<500	1025–950
Cpx inclusions in Pl cores	750–<500	1075–625	1000–925
Large grains of Opx (Cum)	—	1100–725	1025–900
Opx inclusions in Pl cores	925–700	925–700	1050–950
Ilm-Mag pairs*	—	—	1050–980

\* From Wilkinson (1971).

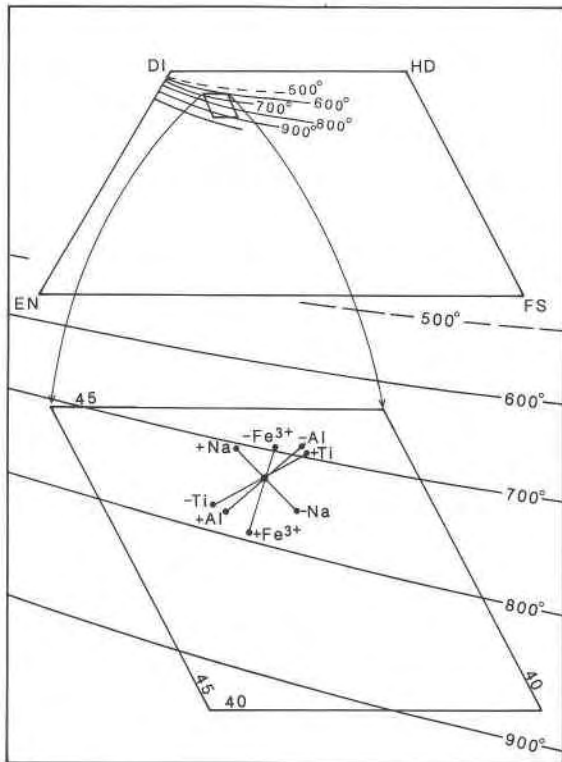


Fig. 5. Effect of variation of minor components in augite analysis 28-071082 (Wo-En-Fs projection and isotherms after Lindsley, 1983). Endmembers for the analysis were recalculated after independent addition and subtraction of 0.2%  $\text{Al}_2\text{O}_3$ ,  $\text{TiO}_2$ , and  $\text{Na}_2\text{O}$ , and 0.02 atoms  $\text{Fe}^{3+}$ . For discussion see text.

900°C, Wyllie, 1977). In addition, Helz (1973) demonstrated that at 5-kbar water pressure it is unlikely plagioclase will persist as restite material in basic source rocks at temperatures  $>850^\circ\text{C}$ .

Although liquidus stability of plagioclase is enhanced by lower water contents of the magma (Dolfi and Trigila, 1983; Merzbacher and Eggler, 1984), the presence of hornblende as an inclusion phase in one of the studied granitoids suggests higher water contents ( $>2$  wt%  $\text{H}_2\text{O}$  at 2 kbar,  $>3$  wt%  $\text{H}_2\text{O}$  at 4 kbar; Merzbacher and Eggler, 1984, Fig. 2).

The interpretation that the pyroxenes have suffered partial equilibration is supported by the presence of exsolution phenomena in the associated Fe-Ti oxides and by the presence of secondary phases including amphiboles, biotite, sericite, and chlorite.

However, equilibration has not proceeded to the stage of generation of pyroxene exsolution lamellae, which are absent. The nature of the equilibration process remains speculative, but the irregular distribution of variably equilibrated compositions in single crystals suggests that the process was quite inefficient under the time, temperature, and fluid conditions of the cooling shallow-crustal magmatic system. Although it was argued above that solid-solid and fluid-solid diffusion processes were unlikely

to have resulted in the bulk compositional similarity of the two parageneses of ferromagnesian phases, these same processes are nevertheless invoked to account for the subtle ranges in composition within individual ferromagnesian phases. The lack of any evidence for re-equilibration in the water-poor volcanic sample further underlines the importance of time (rate of cooling) and fluid conditions in effecting re-equilibration of magmatic ferromagnesian compositions.

Available geologic, mineralogical, and geochemical data support the conclusion that the Barrington Tops granitoids crystallized from hot, relatively dry magmas. That they were hot is suggested by (1) the presence of a narrow pyroxene hornfels contact metamorphic zone (Eggins, 1984), (2) the early crystallization of high-temperature ferromagnesian phases, notably pyroxenes, and (3) relatively low bulk-rock  $\text{SiO}_2$  and high  $\text{MgO}/(\text{MgO} + \text{FeO}_{\text{tot}})$  (see Table 1). That they were relatively dry is suggested by (1) their ascent to shallow crustal levels as indicated by host rocks containing low-grade (burial metamorphic) mineral assemblages (Offler, 1973; Offler and Diessel, 1976; Mason and Kavalieris, 1984) and (2) the early and continued crystallization of anhydrous ferromagnesian phases in both granitoid rock types and late crystallization of biotite without hornblende in one rock type.

The petrographic, chemical, and thermometric data presented here strongly support a magmatic origin for the Barrington Tops plagioclase cores and their ferromagnesian mineral inclusions. The Barrington granitoids are considered, therefore, to have crystallized from magmas that were largely composed of silicate liquid with little or no restite entrained from the source regions. The role of restite appears to be unimportant in the genesis of the Barrington Tops plutons, and caution should be exercised in applying the restite theory of granitoids to all granitoids.

## CONCLUSIONS

1. Plagioclase cores in granitoids of the Permian Barrington Tops Granodiorite contain small ferromagnesian mineral inclusions (orthopyroxene, clinopyroxene, amphibole, and Fe-Ti oxides). Similar textures are observed in volcanic rocks.

2. The inclusions are interpreted to be of magmatic origin. Such inclusions have only been observed in un-doubted magmatic rocks, the inclusion phases match larger discrete ferromagnesian grains, and the inclusions are chemically very similar to analogous larger grains.

3. Application of a new pyroxene thermometer (Lindsley, 1983) reveals a temperature range of  $\sim 1000$ – $<500^\circ\text{C}$  for the Barrington Tops granitoids, indicating partial equilibration of magmatic pyroxenes during slow cooling. By comparison, pyroxenes of a pyroxene dacite range more narrowly ( $\sim 1050$ – $950^\circ\text{C}$ ) owing to rapid quenching.

4. Because the ferromagnesian inclusions are magmatic, it is highly likely that their host plagioclase cores also are magmatic. Cores of granitoid plagioclases cannot therefore be used as unequivocal evidence of "restite" in granitoid genesis.

5. The Barrington Tops granitoids crystallized from magma dominated by silicate liquid, with little or no restite entrained from the source region.

#### ACKNOWLEDGMENTS

The author thanks R. Offer, D. French, and R. H. Vernon for useful discussions and G. B. Johnston and G. Weber for assistance in microprobe analysis. Constructive reviews by T. H. Green, T. N. Grove, and F. J. Spera are appreciated. D. H. Lindsley generously provided a listing of his pyroxene projection program. Final presentation was greatly facilitated by the skills of W. Crebert and J. Walker. The author is grateful for support from the Australian Academy of Science.

#### REFERENCES

- Buddington, A.F., and Lindsley, D.H. (1964) Iron-titanium oxide minerals and synthetic equivalents. *Journal of Petrology*, 5, 310–357.
- Chappell, B.W. (1978) Granitoids from the Moonbi district, New England batholith, eastern Australia. *Geological Society of Australia Journal*, 25, 267–283.
- Czamanske, G.K., and Wones, D.R. (1973) Oxidation during magmatic differentiation, Finnmarka Complex, Oslo area, Norway. Part 2: The mafic silicates. *Journal of Petrology*, 14, 349–380.
- Dolfi, D., and Trigila, R. (1983) Clinopyroxene solid solutions and water in magmas: Results in the system phonolitic tephrite–H<sub>2</sub>O. *Mineralogical Magazine*, 47, 347–351.
- Eggins, S. (1984) Geology and geochemistry of the Barrington Tops Batholith. Univ. N.S.W. B.Sc. Hons. thesis.
- Helz, R.T. (1973) Phase relations of basalts in their melting range at  $P_{H_2O} = 5$  kbar as a function of oxygen fugacity. Part I: Mafic phases. *Journal of Petrology*, 14, 249–302.
- Hensel, H.D., McCulloch, M.T., and Chappell, B.W. (1985) The New England batholith: Constraints on its derivation from Nd and Sr isotopic studies of granitoids and country rocks. *Geochimica et Cosmochimica Acta*, 49, 369–384.
- Kretz, R. (1983) Symbols for rock-forming minerals. *American Mineralogist*, 68, 277–279.
- Leake, B.E. (1978) Nomenclature of amphiboles. *Canadian Mineralogist*, 16, 501–520.
- Lindsley, D. H. (1983) Pyroxene thermometry. *American Mineralogist*, 68, 477–493.
- Lindsley, D.H., and Andersen, D.J. (1983) A two-pyroxene thermometer. *Proceedings of the 13th Lunar and Planetary Science Conference, Part 2. Journal of Geophysical Research*, 88, A887–A906.
- Mason, D.R. (1978) Compositional variations in ferromagnesian minerals from porphyry copper-generating and barren intrusions of the Western Highlands, Papua New Guinea. *Economic Geology*, 73, 878–890.
- Mason, D.R., and Kavalieris, I. (1984) A preliminary note on the Barrington Tops Granodiorite, N.S.W. University of Newcastle, N.S.W., Department of Geology Research Reports #2.
- Merzbacher, Celia, and Egger, D.H. (1984) A magmatic geohygrometer: Application to Mount St. Helens and other dacitic magmas. *Geology*, 12, 587–590.
- Offer, R. (1973) Low grade metamorphism in Carboniferous rocks north of Newcastle. Abstracts, 8th Newcastle Symposium, Geology Department, University of Newcastle.
- Offer, R., and Diessel, C.F.K. (1976) The application of reflectance determinations on coalified and graphitised plant fragments to metamorphic studies. *Geological Society of Australia Journal*, 23, 293–297.
- Piwinski, A.J. (1968) Studies of batholithic feldspars: Sierra Nevada, California. *Contributions to Mineralogy and Petrology*, 17, 204–223.
- Reed, S.J.B., and Ware, N.G. (1975) Quantitative electron microprobe analysis of silicates using energy-dispersive X-ray spectrometry. *Journal of Petrology*, 16, 499–519.
- Spry, A. (1969) *Metamorphic textures*. Pergamon Press, Oxford.
- Vernon, R.H. (1968) Microstructures of high-grade metamorphic rocks at Broken Hill, Australia. *Journal of Petrology*, 9, 1–22.
- (1970) Comparative grain-boundary studies of some basic and ultrabasic granulites, nodules and cumulates. *Scottish Journal of Geology*, 6, 337–351.
- (1983) Restite, xenoliths and microgranitoid enclaves in granites. *Royal Society of New South Wales Journal and Proceedings*, 116, 77–103.
- Vernon, R.H., and Flood, R.H. (1982) Some problems in the interpretation of microstructures in granitoid rocks. In B. Runnegar and P. Flood, Eds. *New England geology*, 201–210. University of New England and AHV Club, Armidale, N.S.W.
- White, A.J.R., and Chappell, B.W. (1977) Ultrametamorphism and granitoid genesis. *Tectonophysics*, 43, 7–22.
- Wilkinson, J.F.G. (1971) The petrology of some vitrophyric calc-alkaline volcanics from the Carboniferous of New South Wales. *Journal of Petrology*, 12, 587–619.
- Wyllie, P.J. (1977) Crustal anatexis: An experimental review. *Tectonophysics*, 43, 41–71.

MANUSCRIPT RECEIVED JANUARY 2, 1986

MANUSCRIPT ACCEPTED JULY 8, 1986